Journal of Applied Electrochemistry **32**: 905–913, 2002.

The influence of different surface conditions in the corrosion process of carbon steel in alkaline sour media☆

E. SOSA[1], R. CABRERA-SIERRA[1,2], M.T. OROPEZA[1] and I. GONZÁLEZ[1,*]
[1]*Universidad Autónoma Metropolitana-Iztapalapa, Depto. de Química, Área de Electroquímica, Apdo. 55-534, C.P. 09340, México D.F., Mexico*
[2]*Escuela Superior de Ingeniería Química e Industrias Extractivas (ESIQIE-IPN) Academia de Química Analítica. Edificio Z5 A.P:75-874, C.P. 07338, México, D.F., Mexico*
*(*author for correspondence, fax: +52 55 58044666, e-mail: igm@xanum.uam.mx)*

Received 22 June 2001; accepted in revised form 9 April 2002

Key words: alkaline sour media, blistered corrosion, carbon steel, EIS, generalized corrosion, surface conditions

Abstract

Different electrochemical methodologies were established to induce general corrosion and blistering on homogeneous and heterogeneous carbon steel surfaces similar to the corrosion damage in a catalytic oil refinery plant. In one case, the film porosity and the iron sulphide stoichiometry were modified and in other case, the surface conditions were changed with sulphur films and microblisters. Additionally, we studied the influence of 1018 carbon steel surface conditions on the corrosion process in a medium simulating the average composition of sour waters in catalytic plants of PEMEX Mexico (0.1 M $(NH_4)_2S$, 10 ppm CN^- as NaCN, pH 8.8). Using the impedance spectra, from 10 kHz to 0.01 Hz, it was possible to qualitatively identify the carbon steel surface condition in an alkaline sour environment and to suggest the same corrosion process steps for this system, despite different surface conditions: charge transfer resistance of steel oxidation in the metal/corrosion product film interface and Fe^{2+} ion and H° diffusion through the corrosion product film. Finally, scanning electron microscopy of a freshly polished surface showed the formation of a homogeneous film immediately after introducing the carbon steel into the sour media. The other surface changes depended on the induced corrosion process and corroborated the electrochemical impedance predictions.

1. Introduction

The evaluation of carbon steel corrosion in alkaline sour media is of great interest to the petrochemical industry, since this phenomenon is responsible for costly economic and human losses. The corrosion process in these media is principally characterized by electrochemical reactions, chemical reactions, formation of insoluble corrosion products that adhere to the metal (non-stoichiometric iron sulphides) [1–4] and blistering corrosion [5–7]. This latter is caused by atomic hydrogen absorption, through the film of corrosion product and the metal. The atomic hydrogen is formed by reduction of the disulphide ions previously adsorbed on either iron or the corrosion product surface. In this case a volume fraction of absorbed atomic hydrogen expands the lattice. Details of this mechanism have been reported in previous work [5, 7]. Corrosion rate determination in alkaline sour media is further complicated by the damage on carbon steel surfaces, such as blistering and generalized corrosion. In general, electrochemical studies for the determination of corrosion rates are carried out using NACE solution (H_2S, NaCl and glacial CH_3OOH, norm TM0177) on a freshly polished surface [8]. However, the effect of metal surface conditions on the corrosion process in these aggressive environments has not been considered.

The objective of this work is to characterize freshly polished surfaces and those showing common (blistered and generalized) damage in sour water refinery environments. For generalized corrosion, two types of film are prepared, one homogeneous and the other heterogeneous. Our approach involves different methodologies to induce damage on the carbon steel surfaces by direct current electrochemical techniques. The films are characterized by electrochemical impedance spectroscopy (EIS) in an alkaline sour medium simulating the average composition of sour waters of condensates in a specific Mexican oil refinery (0.1 M $(NH_4)_2S$, 10 ppm CN^- as NaCN). The characterization study is expected to show physicochemical changes upon modifying the steel surface condition. The election of the characterization

☆This paper was initially presented at the 5th International Symposium on Electrochemical Impedance Spectroscopy at Marilleva, Trento, Italy, June 2001.

medium was based on a previous study that demonstrated the stability of such films in the refinery environment [9]. In this case, this environment is expected to be innocuous enough to guarantee real characterization of nonstoichiometric iron sulphide resulting from the electrochemical oxidation of iron in different media.

2. Experimental details

2.1. *Experimental device description*

A three-electrode cell was used to induce damage on the steel surfaces as well as to characterize them by electrochemical impedance spectroscopy (EIS). All the experiments were performed at room temperature (25 °C). The reference was a mercury/mercurous sulfate electrode saturated with potassium sulfate (SSE), with a value of 0.64 V vs NHE. The working electrode was a clean and damaged 1018 carbon steel surface and the counter electrode was a graphite bar. The reference and counter electrode were contained in separate compartments (Luggin capillary).

2.2. *Preparation of testing specimens*

The working electrode consisted of a 1018 carbon steel disc with a surface area of 0.50 cm^2 (dia. 0.8 cm). This material has a typical composition of 0.14–0.20% C, 0.60–0.9% Mn, 0.035% max. S, 0.030% max P and the rest of Fe. The electrode was embedded in a Teflon base in order to avoid solution filtration within this device. After, a 'curing' with a polyester resin and styrene mixture was carried out. The 'clean' electrode surface was prepared by polishing steel in the following manner: carbon steel electrode surface was polished with silicon carbide emery paper (grade 400) and water, followed by 600 grade emery paper until obtaining a homogeneous surface. The steel surface was then rinsed with acetone. Finally, the specimen was subjected to ultrasonic washing for 5 min in acetone and then used immediately.

2.3. *Preparation of electrolytic media for induction of different surface damages and their characterization*

Table 1 describes the composition of different media and the electrochemical techniques used to induce different surface damage. The solutions described in Table 1 were prepared with deionized water (18.2 MΩ cm) using Merck Analytic-grade Reagents.

For the electrochemical characterization of damaged surfaces a stable electrolytic medium was used. It simulated the average composition of sour waters present in condensates extracted from different equipments of catalytic oil plants of Pemex Mexico (0.1 M $(NH_4)_2S$, 10 ppm CN^- as NaCN, pH 8.8).

2.4. *Damage induction to carbon steel surface*

2.4.1. *Preparation of a blistered corrosion surface*

To induce blistered damage, one 1018 carbon steel electrode was introduced into an alkaline solution (composition in Table 1), at room conditions and without deaeration. This solution was proposed by Wilhem et al. [7] for blister induction. The electrode was treated with cyclic potential pulse applying potential pulses of ±200 mV starting from the corrosion potential (−410 mV vs NHE), 3 s oxidation and 5 s reduction pulse, during 15 min. Cyclic voltammetry was then applied in the cathodic direction starting from the modified corrosion potential (−470 mV vs NHE) during 40 min in a potential interval from −470 to −810 mV vs NHE. The final scan finished at −470 mV. The experiments were performed at room conditions, at a rate of 10 mV s^{-1}.

2.4.2. *Preparation of a surface with a homogeneous film*

To grow a Fe_xS_y film on a clean 1018 carbon steel electrode (freshly polished surface), the electrode was introduced into an alkaline solution (see composition in Table 1), at room conditions and without deaeration. Then, a program of cyclic potentiostatic pulses was applied: a pulse of 5 s at a potential of 200 mV more positive than the corrosion potential (−380 mV vs NHE) and followed by an inverse pulse of 2 s at a potential 200 mV more negative than the corrosion potential. This program was applied for 15 min. The last pulse was finished at −580 mV.

2.4.3. *Preparation of a surface with a heterogeneous film*

To grow a heterogeneous film, one freshly polished carbon steel electrode was introduced into aqueous solution (composition in Table 1), at room conditions and without deaeration. It has been reported [10] that carbon steel, immersed in this environment, forms

Table 1. Electrolytic baths and electrochemical techniques used for inducing the different damage on carbon steel surfaces [6]

Damages	Composition of the electrolytic baths	Electrochemical techniques
Blistered surface	1 M $(NH_4)_2S$, 5000 ppm CN^- (pH = 8.8)	Cyclic potential pulse + cyclic voltammetry
Surface with generalized corrosion (homogeneous film)	1 M $(NH_4)_2S$, 500 ppm CN^- (pH = 8.8)	Cyclic potential pulse
Surface with generalized corrosion (heterogeneous film)	0.04 M $Na_2S_2O_3$	Cyclic voltammetry

the corrosion product with a similar composition of those found in refinery environments. Five voltammetric cycles were applied within an interval from −160 to −760 mV vs NHE, at a rate of 1 mV s^{-1}, in the thiosulfate solution. The corrosion potential of carbon steel in this solution before treatment was −560 mV vs NHE. All solutions were prepared with analytic grade reagents (Merck) and deionized water (Milli- Q^{TM}).

2.5. *Characterization of the corrosion process vs surface conditions*

A clean (freshly polished surface) or damaged electrode (blistered and generalised corrosion) was introduced vertically face down into a solution containing 0.1 M $(NH_4)_2S$, 10 ppm CN^- as NaCN and impedance spectra were measured. The election of characterization media was based on a previous study that demonstrated the stability of homogeneous films in the refinery environment [9]. EIS measurements were made at corrosion potential, applying a sinusoid signal with 10 mV amplitude in a frequency interval from 10 kHz to 10 mHz. The experiments were carried out at room conditions. The impedance diagrams were obtained using a Solartron FRA 1260 frequency response analyser and an EG&G PAR 283 potentiostat. Finally, the SEM studies were based on the surface condition micrographs of the recently induced surface damage. For that purpose a Zeiss DSM 940 A model microscope was used.

3. Results and discussion

3.1. *Selection of the characterization electrolytic medium*

A stability study was carried out tracing EIS diagrams on a homogeneous film (Fe_xS_y), prepared as described in Table 1, at initial time and after 18 h of immersion in different media (sulphide, nitrate, sulphate and borate). This comparative study has already been reported [9], however, this work considered only extreme cases (sulphide and borate media).

Typical Nyquist and Bode diagrams (θ vs log f) obtained at the beginning and the end of the test are shown in Figures 1(a)–(c) and 1(b)–(d), respectively. To avoid the interactions between the film and possible medium-soluble corrosion products (in the case of an unstable film), the last impedance spectrum was performed in a renewed electrolytic solution. The diagrams obtained in the sour medium (Figure 1(a–b)) at the beginning (curve (i)) and the end (curve (ii)) of the test generally show similar behaviour. In the Bode diagram obtained for the film immersed in sulphide medium at the beginning and at 18 h, two time constants are immediately observed (Figure 1(b)) in contrast to a single time constant immediately observed for the borate medium (Figure 1(d)) at both immersion times. On comparing Bode diagrams (Figure 1) at 0 and 18 h of immersion, modifications are observed in the low frequency region that may be associated with the modification of a Fe_xS_y film during immersion. These modifications are more noticeable in borate (Figure 1(d)) than in

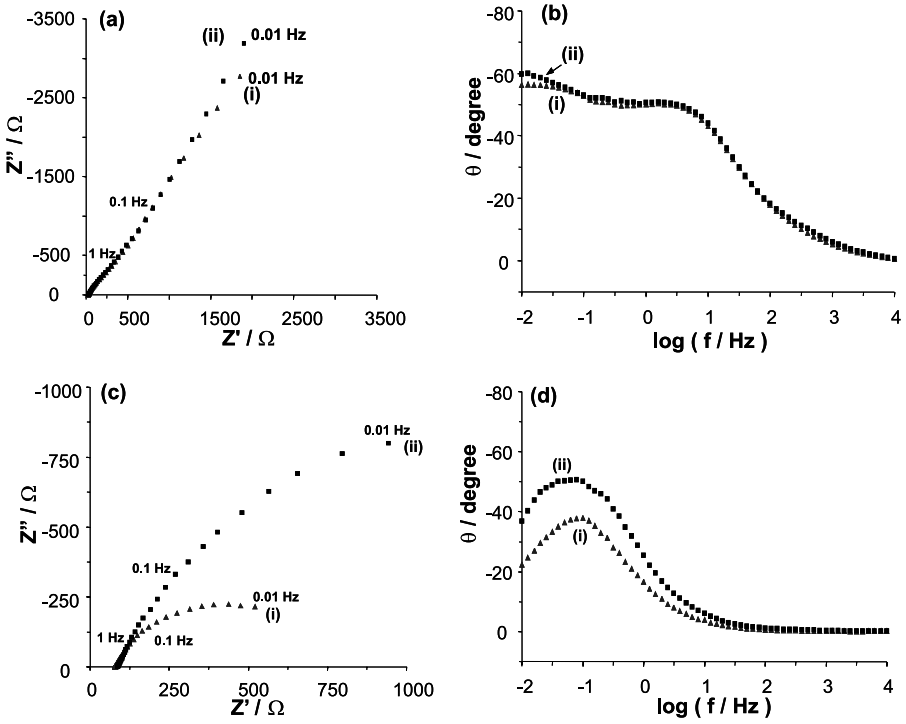

Fig. 1. Typical impedance diagrams obtained at room temperature for homogeneous films (Fe_xS_y) at (i) initial time and (ii) after 18 h immersion in different characterization electrolytic solutions: (a–b) 0.1 M $(NH_4)_2S$ and 10 ppm CN^-, pH 8.8 and (c–d) borate buffer solution (1 M, pH 8.5). (a–c) Typical Nyquist and (b–d) Bode (θ vs log f) diagrams.

sulphide medium (Figure 1(b)), which indicates that Fe_xS_y film is more stable in sulphide medium during immersion. In contrast to studies reported in the literature [11–14] on iron oxide characterization, the borate medium is not appropriate to characterize Fe_xS_y films since these show greater modification in that medium. Details of these stability tests have already been presented [9].

3.2. *Corrosion process studies: superficial conditions*

3.2.1. *Carbon steel surfaces characterization by SEM*

Figure 2 shows the surface micrographs of clean carbon steel (freshly polished surface) (Figure 2(a)), blistered surface (Figure 2(b)) and different surfaces with generalized damage (Figure 2(c) and (d)). These micrographs were obtained before the impedance measurements were

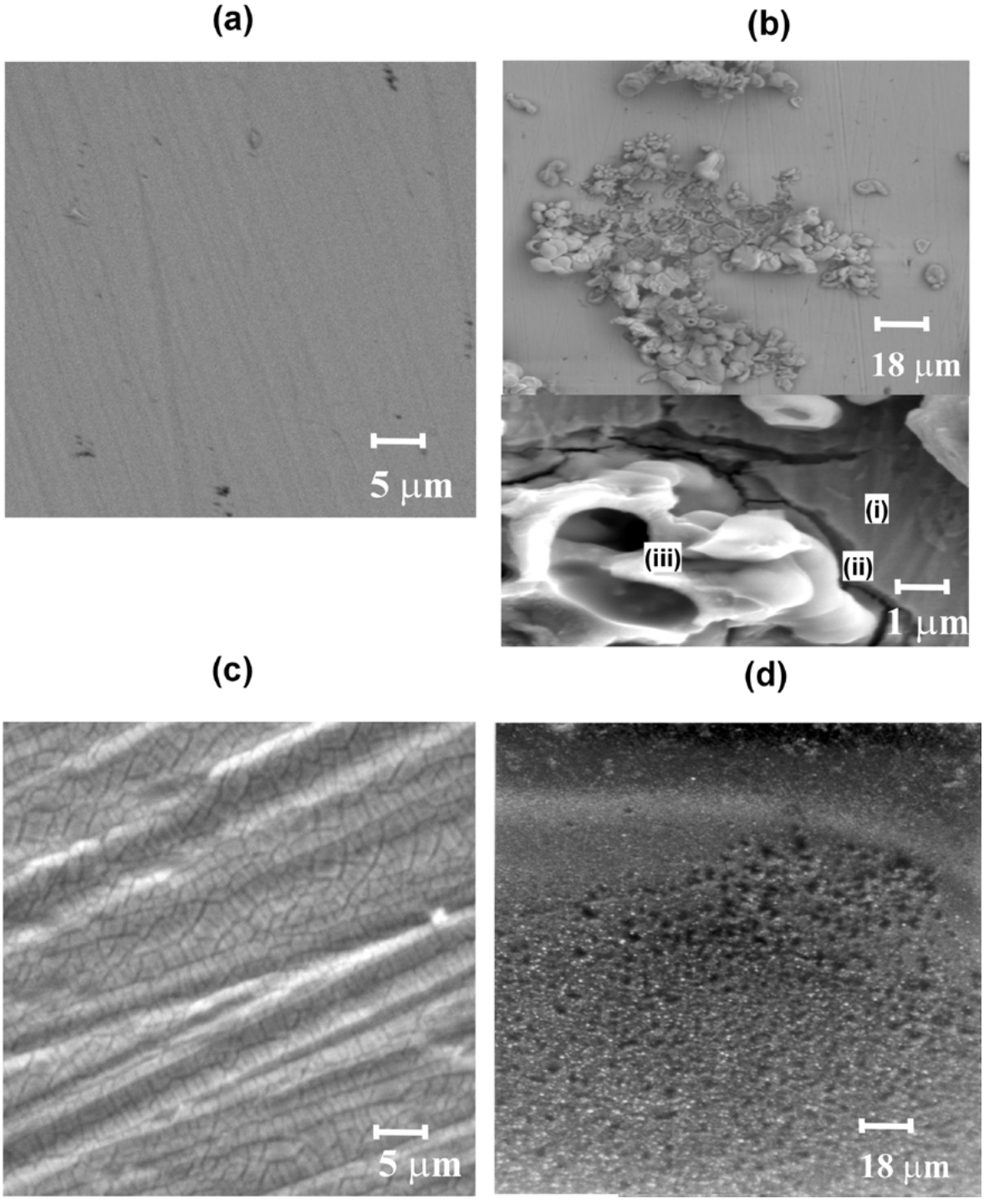

Fig. 2. SEM images of carbon steel surfaces after damage in different electrolytic media before the impedance tests were performed: (a) freshly polished surface, (b) blistered surface induced into 1 M $(NH_4)_2S$, 5000 ppm CN^-, (c) surface with generalized damage induced into 1 M $(NH_4)_2S$ and 500 ppm CN^-, (homogeneous corrosion film) and (d) surface with generalised damage induced into 0.04 M $Na_2S_2O_3$ (heterogeneous corrosion film).

performed. The freshly polished surface shows a homogeneous surface with scratches formed during mechanic polishing. Moreover, the surface of a blistered specimen shows three different zones: one formed by a homogeneous layer of corrosion products (Figure 2(b), zone (i) (nonstoichiometric iron sulphides), another formed by blisters (Figure 2(b), zone (iii) induced by atomic hydrogen diffusion through the film and the third corresponding to cracks around blisters (Figure 2(b), zone (ii) caused by their rupture. Figure 2(c) corresponds to a Fe_xS_y film grown on a carbon steel surface in a concentrated sour medium (Table 1) following the methods described in the experimental section. The surface shows scratches of polishing lines inflicted during the preparation of the steel electrode, indicating the film thickness; likewise a fragmented surface can also be observed. Previous studies on the evolution of this film assumed the existence of two regions [4]. The first internal region is compact and homogeneous, while the external is fragmented. In this latter, the fragmented phase formation may be attributed to the dehydration of the film occurred in the vacuum camera when SEM study was carried out. Finally, the Figure 2(d) corresponding to a Fe_xS_y film grown on a carbon steel surface in thiosulphate medium (Table 1) shows only one morphology consisting of porous nonhomogeneous precipitates (Figure 2(d)). In this paper, they are labelled as homogeneous (Figure 2(c)) and heterogeneous (Figure 2(d)) surfaces.

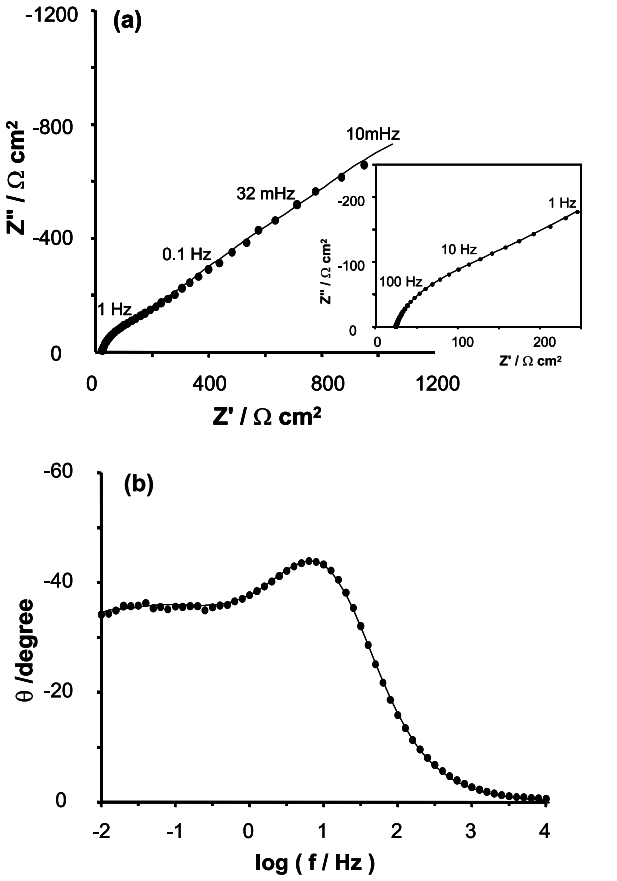

Fig. 3. EIS diagrams for a 1018 carbon steel surface (freshly polished surface) obtained in a solution 0.1 M $(NH_4)_2S$ and 10 ppm CN^-, at room temperature, pH 8.8. Continuous lines correspond to the adjustment using equivalent circuit of Figure 8(a) and dots correspond to experimental values.

3.2.2. *Characterization by electrochemical impedance spectroscopy*

Figures 3–6 show Nyquist and Bode diagrams of each of the cases studied. In general, for Nyquist diagrams (Figures 3–6(a)) two loops are immediately observed corresponding to low and intermediate frequencies, respectively. At higher frequencies (Figures 3–6(a), inset) a third time constant appears. The differences observed in impedance values as well as in the shape of loops and the time constants show clearly the effect of surface condition in the corrosion process. Likewise, Nyquist diagrams reflect a considerable modification in Z' and Z'' values for different surfaces. In Bode diagrams (Figure 3–6(b)), which show more sensitive changes, two time constants are immediately observed on the clean (Figure 3(b)), blistered (Figure 4(b)) and homogeneous film (Figure 5(b)) surfaces, while for the heterogeneous film (Figure 6(b)), only one is immediately observed. For frequencies higher than 100 Hz a third time constant is slightly visible.

Figure 3(a) corresponds to the Nyquist diagram for impedance values of the clean (freshly polished surface) carbon steel electrode. Three loops are observed, one better defined at intermediate frequencies ($1 < f <$ 100 Hz), an other less defined at high frequencies ($f >$ 100 Hz) and the third observed at low frequencies ($f <$ 0.1 Hz). On the Bode diagram (Figure 3(b)), three time constants are observed, one at 6.3 Hz, the other less defined, at approximately 0.04 Hz and the third time constant, lesser defined at $f >$ 100 Hz.

Figure 4(a) shows the Nyquist diagram corresponding to a blistered surface. This spectrum, show a similar trend to that found on a clean surface, except for higher impedance values for the same frequency interval. Figure 5(a) shows the Nyquist diagrams obtained on the homogeneous film. This spectrum is similar to that of the blistered surface, but with a considerable decrease in Z' values. Regarding the Bode diagram corresponding to the homogeneous surface (Figure 5(b)), three time constants are observed as in those for clean and blistered surfaces (Figures 3(b) and 4(b)). They appear practically at the same frequencies, but are better defined in blistered and homogeneous surfaces. This means that the same phenomena occur on both surfaces during the corrosion process. The time constant observed at 10 Hz has a higher phase angle at the blistered surface, whereas at the clean surface its value diminishes. However, the time constant observed in the low frequency region ($f <$ 0.5 Hz), has a higher phase angle value when the steel surface has a homogeneous film (Figure 5(b)).

Figure 6(a) corresponds to impedance values of a surface with a heterogeneous film. Two loops are immediately observed, one at high frequency (100 Hz, Figure 6(a), inset) and the other, at low frequency

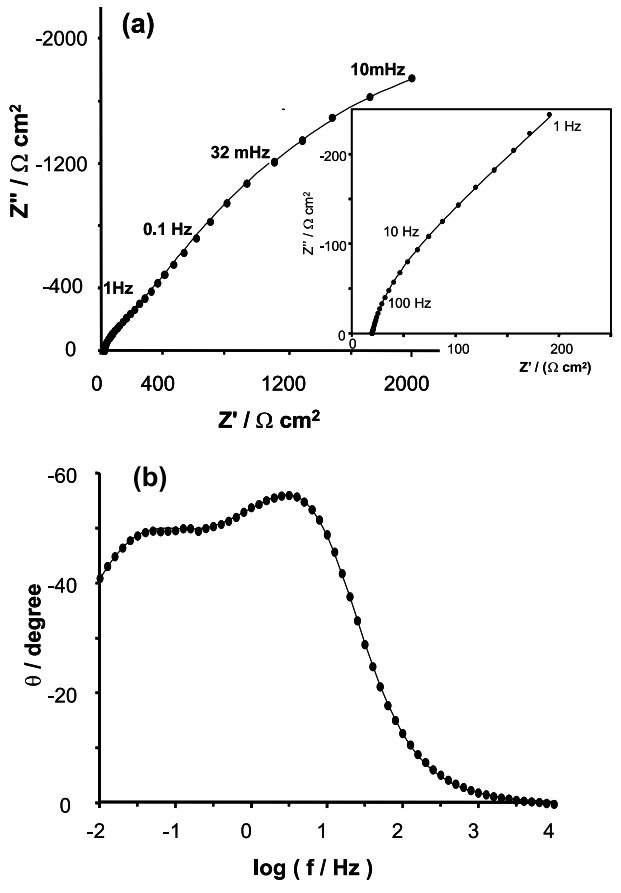

Fig. 4. EIS diagrams for a blistered carbon steel surface obtained in a solution 0.1 M $(NH_4)_2S$ and 10 ppm CN^-, at room temperature, pH 8.8. Continuous lines correspond to the adjustment using equivalent circuit of Figure 8(a) and dots correspond to experimental values.

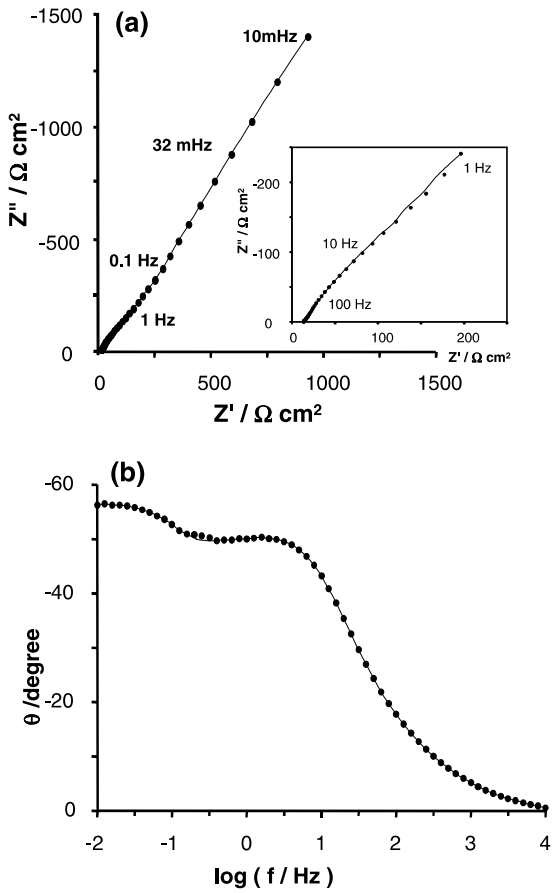

Fig. 5. EIS diagrams carbon steel with homogeneous corrosion film obtained in a solution 0.1 M $(NH_4)_2S$ and 500 ppm CN^-, at room temperature, pH 8.8. Continuous lines correspond to the adjustment using equivalent circuit of Figure 8(a) and dots correspond to experimental values.

($f < 0.5$ Hz). The loop at intermediate frequencies is difficult to observe. This spectrum also has lower impedance values in relation to other spectra by one order of magnitude. In addition, Figure 6(a) shows the capacitive loop at high frequencies (see inset of Figure 6(a)), which is not observed in other cases due to the magnitude of the impedance values. This is basically the consequence of the high impedance values displayed by the other surfaces. In the Bode diagram (Figure 6(b)) of the heterogeneous surface, one time constant is observed in the low frequency region (0.07 Hz) as in the other three surfaces. However, the time constant observed in the intermediate frequency region ($1 < f < 100$ Hz) diminishes considerably.

These diagrams show a similar trend, except for the time constants and their respective impedance values that are modified for the same frequency interval. This may be due to either a variable thickness of corrosion product films during their growth or their different nature. It is important to emphasise that in all studied cases the EIS diagrams show two easily identifiable time constants; however a third time constant present at $f > 100$ Hz is hardly identifiable. To identify this time constant we made a graph like that proposed by Orazem [15] but considering first derivative criterion. Figure 7 shows an example of this plot corresponding to the blistered surface. In this Figure, three minima related to three time constants can be clearly observed.

Since the characterization was carried out in the same environment and the diagrams showed the same number of time constants, the corrosion process mechanisms of the four surfaces proved to be similar. Therefore, physicochemical properties of the interface (film–medium) are the only factor that determines the corrosion process kinetics. Considering the above, the impedance spectra analysis was carried out fitting the experimental data to the equivalent circuit models of Figure 8 using nonlinear regression [16].

These models (Figure 8) described the corrosion process on carbon steel in alkaline sour media [4–6]. Continuous lines in Figures 3–6 represent the fit to the (Nyquist and Bode) impedance diagrams using the circuits shown in Figure 8. These Figures demonstrate good fit between the proposed circuits and the experimental data. Table 2 summarizes the parameter values for the circuits obtained by the best fit to the experimental impedance diagrams.

The solution resistance (R_s) values of 17 Ω cm^2 (not shown in Table 2) were similar in all surfaces studied. Table 2 shows different values of electric elements obtained in the test of different damaged surfaces. This

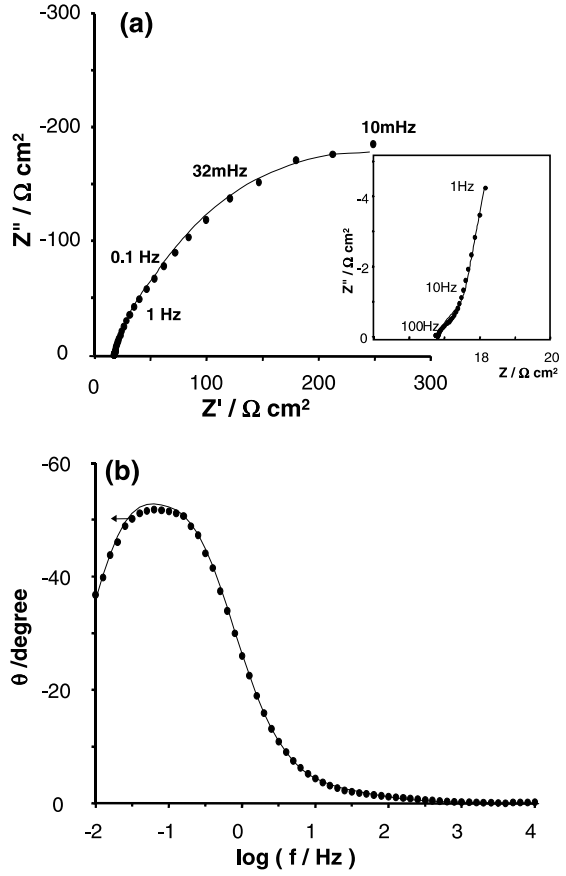

Fig. 6. EIS diagrams carbon steel with heterogeneous corrosion film obtained in a solution 0.1 M $(NH_4)_2S$ and 10 ppm CN^-, at room temperature, pH 8.8. Continuous lines correspond to the adjustment using equivalent circuit of Figure 8(b) and dots correspond to experimental values.

fact indicates that the stages involved in the corrosion process are modified by the surface condition. The resistance value, R_1 is three orders of magnitude smaller than R_3 and two orders of magnitude than R_2, thus indicating the difference of velocity at which the processes associated with these parameters are carried out.

It is important to emphasise that the equivalent circuits described in Figure 8 have also been used to describe EIS diagrams obtained on highly porous surfaces of corrosion products [17, 18]. In these cases, R_1 was associated with the resistance of the film formed, whereas R_2 corresponds to the charge transfer onto the uncovered metallic surface. According to the data of Table 2, this phenomenological description is not applicable to the surfaces studied here. On the basis of additional experiments [4–6, 9], we have associated the Figure 8(a) circuit with different stages of the corrosion process in sour media. This model considers the following variables: solution resistance (R_s), double-layer capacitance (C_{dl}), charge transfer process (R_1) at the metal–Fe_xS_y film interface and a further contribution due to the Fe^{2+} ion and atomic hydrogen diffusion, R_2–Q_2 and R_3–Q_3 arrangements, respectively [4–6].

The R_1 values had a variation of 3.5–34 Ω cm^2. These are in agreement with those reported by Vedage et al. [19] of 5–10 Ω cm^2 for a carbon steel–sour media interface in acidic pH, as well as with other values reported in the literature [4–6] related to the carbon steel–corrosion products–alkaline sour media interface. The values of R_2 and R_3 are comparable to those reported in the literature for the metal/corrosion products/sour media interface [4–6, 9].

3.2.3. *Pseudocapacitance analysis*

Pseudocapacitance values were determined from the constant phase element value (Y_0) (Table 2) using Equation 1 [20]:

$$C_{HF} = \frac{(Y_0 R_{HF})^{1/n}}{R_{HF}} \quad (1)$$

The values obtained for a freshly polished surface and homogeneous film were 88 and 96 μF cm^{-2}, respectively. These are of the same order of magnitude as those reported for the metal–solution interface [21], which means that the freshly polished carbon steel surface and homogeneous film–alkaline sour medium interfaces

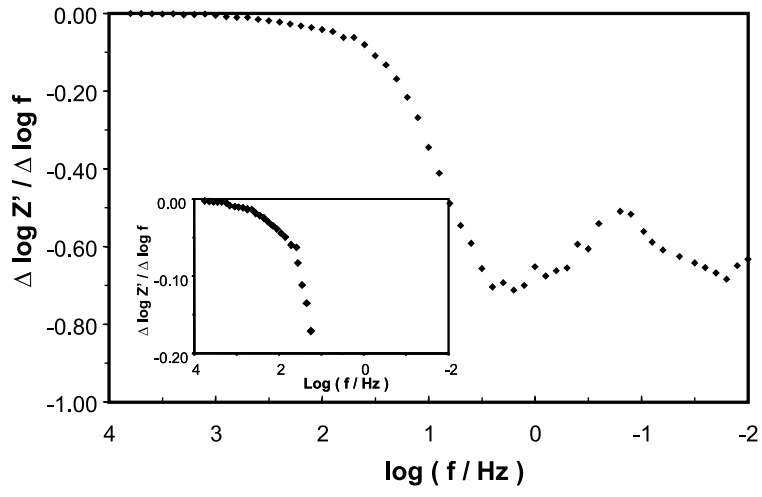

Fig. 7. Curve $\Delta \log Z'/\Delta \log f$ vs $\log f$ obtained from EIS data corresponding to a blistered surface.

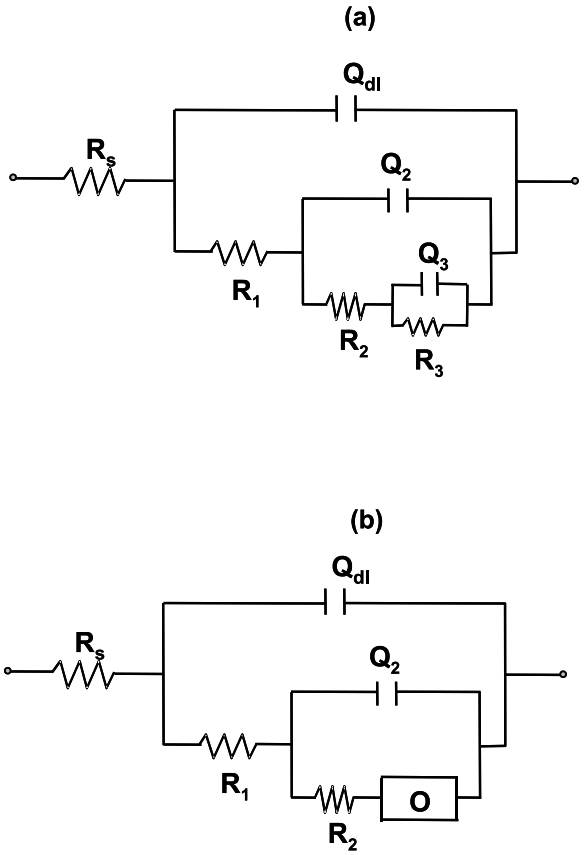

Fig. 8. Equivalent circuits describing the corrosion of carbon steel with different surface damage in alkaline sour media. (a) Freshly polished surface, blistered surface and carbon steel with homogeneous corrosion film, (b) carbon steel with heterogeneous corrosion film.

have ideal behaviour. For the blistered surface, this value was 400 μF cm^{-2}, one order of magnitude greater than that of the freshly polished surface and related to the increase in thickness of the film formed during blister induction (Figure 2(b)). The high pseudocapacitance value (5898 μF cm^{-2}), obtained for the surface with generalized damage (heterogeneous film), is of the same order of magnitude as those reported by Bonnel [22] for interfaces with a film of corrosion products (oxide). Bonnel's studies reported high capacitance values (500–1750 μF) for the corrosion products formed on the substrate that displayed porous and conducting characteristics. In our work the porous characteristic are clearly supported by SEM (Figure 2(d)) and the conducting characteristic is certainly due to the nonstoichiometric iron sulphide mainly composed of corrosion product [4, 5, 19]. However, the values obtained in this work are notably high than those reported by Bonnel. These values suggest either a mass transfer process or a faradaic pseudo-capacitance. A deeper study may be performed to elucidate this phenomenon. The differences in pseudocapacitance parameters for damaged surfaces are due to the change in surface roughness and the nature of the corrosion product film.

3.2.4. *Charge transfer resistance analysis*

Regardless of the carbon steel surface condition (freshly polished and generalized corroded surface), the R_1 values (Table 2) are of the same order of magnitude indicating that R_1 effectively corresponds to the charge transfer reaction at the metal–corrosion products interface. We have previously shown that the thick corrosion film was immediately formed when a freshly polished surface was immersed in the alkaline sour media [5]. However, for the blistered surface the value obtained is one order of magnitude greater. This is due to either a lack of precision in the evaluation of this resistance as a consequence of high impedance values, or to a modification in a surface work function caused by the introduction of H° to the lattice.

3.2.5. *Analysis of Fe^{2+} ion diffusion process*

As mentioned above, the electric arrangement R_2–Q_2, corresponds to Fe^{2+} ion diffusion through the corrosion product films. The values for R_2 for different surfaces, shown in Table 2, are of the same order of magnitude. The R_2 value for the freshly polished surface is 278 Ω cm^2, 1.12 times smaller than the R_2 value for the blistered surface, whereas for the surface with generalized damage it diminishes by a half. This variation in resistance may be due to the thickness of the film of corrosion products formed during damage induction which is different in each case, or to the fact that alkaline sour medium, used for damage induction,

Table 2. Values for the electric circuit elements (Figure 8) used for best fit to the impedance diagrams of the carbon steel surface–alkaline sour environment interface, as a function of carbon steel surface conditions

Surface states	Q_{dl}		R_1/Ω cm^2	Q_2		R_2/Ω cm^2	Q_3		R_3/Ω cm^2
	$Y_0 \times 10^4$/Siemens	n		$Y_0 \times 10^5$/Siemens	n		$Y_0 \times 10^5$/Siemens	n	
Freshly polished surface	4.9	0.70	3.5	18	1	278	15.5	0.54	3707
Blistered surface	3.7	0.86	34	2.9	1	313	8.1	0.65	6656
Surface with generalised corrosion (homogeneous film)	0.48	1	3.5	78	0.7	516	7.8	0.72	18 800
	Q_{dl}		R_1/Ω cm^2	Q_2		R_2/Ω cm^2	O		$b/s^{1/2}$
	$Y_0 \times 10^4$/Siemens	n		$Y_0 \times 10^4$/Siemens	n		$Y_0 \times 10^3$ S		
Surface with generalised corrosion (heterogeneous film)	63	0.82	2.54	34	1	136	6.4	3.9	

was different from that used for the characterization. On the other hand, the decrease in the R_2 parameter for the surface with a heterogeneous corrosion film is due to increase in film porosity (see Figure 2(d)).

3.2.6. *Analysis of H° diffusion process*

In Bode diagrams (Figures 3–6(b)), the time constant observed in the low frequency region corresponds to atomic hydrogen diffusion through the film, represented in the equivalent circuit with a parallel arrangement (R_3–Q_3). In each case, the resistance values, R_3, (Table 2) are different, which indicates the different physicochemical nature of the films adhering to the substrate. The increase in the magnitude of R_3 for blistered and homogeneous surfaces, as compared to a freshly polished surface, is due to the more compact film formed during damage induction (Figure 2). In the surface with a heterogeneous film, this value diminishes considerably and the R_3–Q_3 arrangement is modified to the limiting case where $n = 0.5$, which corresponds to a linear diffusion element (O). The diffusion resistance value (R_3) calculated through the relationship between b and Y_0 values (Table 1) was 297 $\Omega\,cm^2$ and is of the same order of magnitude as R_2. This similarity is due to the increase in porosity of the film for the surface with generalized damage (heterogeneous film, see Figure 2(d)).

4. Conclusions

In these studies, different electrochemical methodologies were established to induce damage common in catalytic oil refinery plants (blistering and general corrosion) on carbon steel surfaces. We studied the influence of 1018 carbon steel surface conditions on the corrosion process in alkaline sour media prepared to simulate the average composition of sour waters in catalytic plants of Pemex Mexico (0.1 M $(NH_4)_2S$, 10 ppm CN^- as NaCN, pH 8.8).

The election of characterization media was based on a previous study which demonstrated the stability of homogeneous films in the refinery environment [9]. According to impedance spectra, from 10 kHz to 0.01 Hz, it was possible to qualitatively identify the carbon steel surface condition in an alkaline sour environment. It was also found that the corrosion process for all surface conditions presents the same stages: charge transfer resistance of steel oxidation at the metal–corrosion product film interface and Fe^{2+} ion and H° diffusion through the corrosion product film.

Additionally, it was demonstrated that when there was no damage to the surface (freshly polished surface), a homogeneous film was formed instantaneously upon introducing the carbon steel into the sour media. When the surface shows blistered corrosion, the impedance values increase. After damaging the surface additionally by growing a heterogeneous film, the impedance values diminish and atomic hydrogen diffusion is more favoured.

Acknowledgements

E. Sosa and R. Cabrera-Sierra are grateful to Conacyt and FIES for their postgraduate grants. The authors acknowledge financial aid from Conacyt (project 32689 E) and FIES 98-13-II.

References

1. T. Hemmingsen and H. Lima, *Electrochim. Acta* **43** (1998) 35.
2. R.C. Newman, K. Rumash and J. Webster, *Corros. Sci.* **33** (1992) 1877.
3. Z.A. Foroulis, *Corros. Prevent. Control* Aug. (1993) 84.
4. E. Sosa, R. Cabrera-Sierra, M.E. Rincón, M.T. Oropeza and I. González, *Electrochim. Acta* **47** (2002) 1197.
5. R. Cabrera-Sierra. I. García, E. Sosa, M.T. Oropeza and I. González, *Electrochim. Acta* **46** (2000) 487.
6. E. Sosa, R. Cabrera-Sierra, M.T. Oropeza and I. González, *Corros. Sci.* **44** (2002) 1515.
7. S.M. Wilhem and D. Abayarathna, *Corrosion* **50** (1994) 152.
8. TM0177-90, 'Standard Test Method-Laboratory Testing of Metals for Resistance to Sulfide Stress Cracking in H_2S Environments', Houston, TX, NACE (1990).
9. E. Sosa, R. Cabrera-Sierra, M.T. Oropeza and I. González, *Corrosion* **58** (2002).
10. S. Tsujikawa, A. Miyasaka, M. Veda, S. Ando and T. Yamada, *Corrosion* **49** (1993) 409.
11. M.I. Nagayama and M. Cohen, *J. Electrochem. Soc.* **109** (1962) 781.
12. B. MacDougall and J.A. Bardwell, *J. Electrochem. Soc.* **135** (1988) 2437.
13. A.J. Davenport and M. Sansome, *J. Electrochem. Soc.* **142** (1995) 725.
14. M.P. Ryan, R.C. Newman and G.E. Thompson, *J. Electrochem. Soc.* **142** (1995) L177.
15. M. Orazem, 2001 ECS and ISE Joint International Meeting, EIS course, San Francisco, USA, Sept. (2001).
16. B.A. Bouckamp, 'Users Manual Equivalent Circuit', vers. 4.51, Faculty of Chemical Technology, University of Twente, The Netherlands (1993).
17. K. Juttner, W. Lorentz and W. Paatsch, *Corros. Sci.* **29** (1989) 279.
18. J. Pang, A. Briceno and S. Chander, *J. Electrochem. Soc.* **137** (1990) 3447.
19. H. Vedage, T.A. Ramanararanan, J.D. Mumford and S.N. Smith, *Corrosion* **49** (1993) 114.
20. M.A. Pech-Canul and L.P. Chi-Canul, *Corrosion* **55** (1999) 948.
21. J.R. Macdonald, 'Impedance Spectroscopy Emphasizing Solid Materials and Systems' (J. Wiley & Sons, New York, 1987), 99–103.
22. A. Bonnel, F. Dabosi, C. Deslouis, M. Duprat, M. Keddam and B. Tribollet, *J. Electrochem. Soc.* **130** (1983) 753.